Development of a chitosan-montmorillonite nanocomposite film containing *Satureja hortensis* essential oil

V. Alizadeh[1], H. Barzegar[2*], B. Nasehi[3], V. Samavati[2]

Abstract

The present work describes the physicochemical and antimicrobial properties of active films developed by incorporating different concentrations (0.5, 1, and 2% v/v) of *Satureja hortensis* essential oil (SEO) and 3% (w/w) nanoclay into a chitosan- montmorillonite nanocomposite film. The tensile strength (TS) of the films significantly decreased and elongation at break (EAB) increased with the incorporation of SEO. The control film exhibited the lowest water vapor permeability. In addition, decreases in water solubility (WS) and transparency were observed with increasing the concentration of SEO. Thermogravimetric analysis (TGA) indicated that films incorporated with SEO exhibited a higher degradation temperature compared with the control. The structural properties and morphology of the nanocomposite films were examined by X-ray diffractometry (XRD) and Scanning electron microscopy (SEM). SEO-incorporated films were more effective against gram positive bacteria (*Staphylococcus aureus* and *Bacillus cereus*) than gram negative ones (*Salmonella typhimurium* and *Escherichia coli*). The results suggested that SEO, as a natural antibacterial agent, has the potential to be applied in antimicrobial biodegradable films.

Keywords: Nanocomposite film, Chitosan, *Satureja hortensis*, Essential oil, Antimicrobial.

Introduction

Compared to plastic packaging materials, application of biopolymer-based films for shelf-life extension purposes has grown extensively in the last 20 years due to their environmental advantages. Biopolymer-based edible films and coatings can also act as a barrier to external influences such as moisture, carbon dioxide, oxygen, lipid and mechanical property modifiers, as a carrier for food additive in food systems (Gennadios, Hanna, & Kurth, 1997). Materials available for developing edible films usually based on polysaccharides, proteins and lipids (Peng, & Li, 2014). Chitosan, a deacetylated (to varying degrees) product of chitin, is the second most abundant natural biopolymer after cellulose. Compared to other polysaccharides, chitosan has several advantages, such as non-toxicity,

biodegradability, biocompatibility and biofunctionality (Abdollahi, Rezaei, & Farzi, 2012). However, weak mechanical and gas barrier properties, and poor water resistance limit its further applications, particularly in the presence of water and humid environments (Wang *et al*., 2005; Xu, Ren, & Hanna, 2006). Nanocomposites are one of the most promising options to improve the mechanical, barrier and thermal properties of films made from biopolymers (Avella *et al*., 2005). Development of polymer/layered silicate nanocomposites is one of the latest revolutionary steps of the polymer technology. Incorporation of nanoparticles into biopolymers in low percentages improves their mechanical strength, heat resistance, and barrier characteristics and thus can broadly be used for diverse applications, specifically packaging needs (Zolfi, Khodaiyan, Mousavi & Hashemi, 2014). Montmorillonite (MMT) is the most prevalent and important nano-clay used layered silicates because it is eco-friendly and easily accessed in large amounts with relatively low cost. Therefore, it is possible to improve the properties of chitosan films through the addition of small amounts (2–8%)

1, 2 and 3. MSc. Student, Assistant Professor and Associate Professor, Department of Food Science and Technology, Ramin Agriculture and Natural Resources University of Khuzestan, Iran.
(*-Corresponding Author: hbarzegar@ramin.ac.ir)

of MMT (Almasi, Ghanbarzadeh & Entezami, 2010). Another approach to improve the functional characteristics of the biopolymer-based films is to activate them with various types of additives such as antimicrobial agents to increase the shelf-life of foods. Currently, the use of natural active antimicrobials, such as plant extracts, instead of synthetic preservatives appears to be an attractive option (Atef, Rezaei, & Behrooz, 2015). Plant essential oils are major sources of phenolic compounds and have been indicated to have a wide range of antimicrobial effects (Shen & Kamdem, 2015). *Satureja hortensis* (or commonly known as Summer Savory) is a well-known medicinal plant, annual and aromatic herb belonging to the *Lamiaceae* family, which is widely cultivated in the Mediterranean region. It has shown antispasmodic, antidiarrheal, antioxidant and good antimicrobial properties (Hadian, Ebrahimi, & Salehi, 2010; Shojaee-Aliabadi *et al.*, 2013). Phenols, carvacrol and thymol as well as p-cymene, b-caryophyllene, linalool and other terpenoids are the major active constituents of *Satureja hortensis* essential oil (SEO) (Sefidkon, Abbasi, & Khaniki, 2006). The antimicrobial effect of SEO has been reported in several studies (Shojaee-Aliabadi *et al.*, 2013; Atef *et al.*, 2014; Sefidkon *et al.*, 2006). Thus, the incorporation of SEO into chitosan films offers the probability not only for imparting bioactivity (e.g. antimicrobial and antioxidant activity), but also improving the physicochemical properties of films. To the best of our knowledge, no specific study has been done on the incorporation of SEO into nanocomposite films based on chitosan and MMT. Hence, this work was carried out to evaluate SEO effects on the properties of chitosan/MMT nanocomposite films. The characterizations included the mechanical properties, water barrier ability, optical attributes, microstructural and thermal behavior as well as antimicrobial activity of the films against *S. aureus*, *B. cereus*, *E. coli* and *S. typhimurium*.

Materials and methods

Crab shell chitosan with the deacetylation degree of 75–85% (medium molecular weight) was purchased from Sigma–Aldrich Chemical Co., USA. Unmodified natural MMT (Cloisite Na+) was purchased from Southern Clay Products (USA). Calcium chloride (analytical grade), Tween 80, Glacial acetic acid and Glycerol were supplied from Merck, Germany. Sodium chloride was obtained from Dr. Mojallai (Tehran, Iran). Mueller–Hinton agar (MHA) and Mueller–Hinton Broth (MHB) were provided from Merck Co. (Darmstadt, Germany). *Satureja hortensis* essential oil was bought from Barij Essence Pharmaceutical Co. (Kashan, Iran), and stored in a sealed dark container at 6 °C until the day of experiments.

Bacterial strains

The bacterial strains used in the present study included *Staphylococcus aureus* (ATCC 25923), *Bacillus cereus* (PTCC 1154), *Salmonella typhimurium* (ATCC 14028) and *Escherichia coli* (PTCC 1330). All the stock cultures were provided by Persian Type Culture Collection (Tehran, Iran). Stock cultures of the studied bacteria were reserved in Brain Heart Infusion Broth (BHI) and kept at -20°C before the tests. Subculturing was conducted every 30 days to preserve bacterial viability.

Preparation of the antimicrobial films

Chitosan solutions were prepared through the casting method proposed by Abdollahi *et al.* (2012) with some modifications. Film solution with the concentration of 2% (w/v) was prepared by dissolving crab shell chitosan in a 1% (w/v) aqueous acetic acid solution while mixing vigorously at 1250 rpm on a magnetic stirrer set at 90°C for about 20 min. After dissolution, glycerol was added as a plasticizer at 30% content based on dry chitosan film. The montmorillonite (3% w/w on solid polymer), was dispersed in 1% (v/v) aqueous acetic acid solution and vigorously stirred for 6 h. The obtained mixture was sonicated for 30 min at room temperature. The

clay dispersion was added to the aqueous acetic acid dispersion of chitosan and stirring was continued for 4 h. Tween 80 at 0.2% of SEO (v/v) was added as oil dispersant. Stirring was continued for a further 30 min at 40°C after the addition of the emulsifier. Finally, SEO was incorporated into the film forming solution at the final concentrations of 0.5, 1 and 2% (v/v) of the chitosan solution. Homogenization was performed by Ultra Turrax homogenizer (IKA T25-Digital Ultra Turrax, Staufen, Germany) at 13,500 rpm for 3 min. The filmogenic solution was then stirred slowly for 10 min to remove all air bubbles. Finally the film solution was cast on Plexiglas plate and dried for 30 h in an oven (35°C). Dried films were preconditioned in desiccators containing saturated solutions of Ca $(NO_3)_2$, $6H_2O$ (at 25°C and 53% relative humidity) until evaluation. All samples were prepared in triplicate.

Film thickness measurement

Thickness of the film was measured using a manual digital micrometer (Mituto, Tokyo, Japan) having a sensitivity of 0.001 mm, at 8 random locations. The mean value was used for the calculation of tensile strength (TS) and water vapor permeability (WVP).

Water solubility

The film solubility in water was determined from immersion assay under constant agitation in distilled water for 6 h, according to the method suggested by Hosseini *et al.* (2009). After filtration, the undissolved film was dried at 110°C to reach a constant weight (final dry weight). The initial dry weight of the samples (1 cm ×3 cm) was determined by drying at 110°C to reach a constant weight. The difference between the initial and final dry weights was reported as solubility.

Water vapor permeability (WVP)

WVP tests were performed at 25°C and 75% RH gradient based on ASTM E96 gravimetric method (Shojaee-Aliabadi et al. 2013). Briefly, the glass permeation cups with the internal diameter of 3 cm and depth of 3.5 cm, containing anhydrous calcium chloride

(desiccant 0% RH), were sealed by the test films. The film-covered cups were stored in a desiccator containing the sodium-chloride-saturated solution. The weight gain of the test cups was recorded in 6 h intervals over a 48 h period. The difference in RH corresponding to a driving force of 1753.55 Pa, was expressed as water vapor partial pressure. The water vapor transmission rate (WVTR) of the films was measured from the slope reached by linear regression analysis (weight change vs. time) of moisture weight gain (Δm) transferred through an effective film area (A) during a certain time (Δt), once the stationary state (linear) was obtained. WVTR and WVP were calculated using the following equations:

$$\text{WVP} \ (10^{-10} \text{ g/m s Pa}) = \frac{WVTR \times X}{P(R1 - R2)} \qquad (1)$$

$$\text{WVTR} = \frac{\Delta m}{A \times \Delta t} \qquad (2)$$

where X is the average film thickness (mm), P(R1− R2) is the water vapor pressure differential across the film (Pa), R1 is the relative humidity in the desiccator (75%) and R2 is the relative humidity in the cup (0%). All tests were performed in three replicates.

Mechanical properties

Tensile strength (TS, MPa) and elongation-at-break (ELB, %) were performed at 25°C and 53% RH by a Texture Analyzer (TA-XT-plus Stable Micro Systems, Surrey, UK), according to ASTM (D882-02, 2002) standard. In order to prepare the samples, films were cut into 1 ×6 cm^2 strips. All tested film strips were fixed with an initial grip separation of 40 mm and stretched at a crosshead speed of 0.83mm/s until breaking.

Optical properties

Color values of the film samples were determined using a CR-400 series colorimeter (Minolta, Tokyo, Japan). Measurements were expressed as lightness (L), redness (a) and yellowness (b). Color measurements were done on white standard backgrounds (L*=92.23, a*=−1.29, and b*=1.19). Prior to optical measurements, the films were conditioned in desiccators at 53 % RH. At

least, three points of each film specimen were selected randomly to measure the optical properties of the chitosan films. The total color difference (ΔE) and the whiteness index (WI) were calculated as follows:

$$\Delta E = \sqrt{(L* - L)^2 + (a* - a)^2 + (b* - b)^2} \quad (3)$$

$$WI = 100 - \sqrt{(100 - L)^2 + a^2 + b^2} \quad (4)$$

Where L*, a*, and b* are the color parameters of the standard plate and L, a, and b are the color parameters of the sample.

X-ray diffraction (XRD)

XRD measurements were perform using a Philips X'Pert MPD Diffractometer (Eindhoven, Netherlands), operating at Cu Kα wavelength of 1.544 nm, at 40 kV and 30 mA. Nanocomposite films were scanned in the angular region (2Θ) of 1–12°, speed of 1°min⁻¹ at room temperature.

Scanning electron microscopy (SEM)

SEM images of the surface and cross-section of the film samples were captured by a SEM apparatus (KYKY–EM3200, China). The film samples were fixed on the support using the double side adhesive tape and then mounted on the specimen holder. The films were coated with gold by sputter coater (Model: KYKY–SBC12, China) under vacuum condition. The samples were scanned using an accelerating beam voltage of 22 kV.

Thermogravimetric (TGA) analysis

Thermogravimetric analysis of the films was carried out using a Thermal Analyzer (TGA7, PerkinElmer, Norwalk, CT, USA) from 25 to 550 °C at a heating rate of 10 °Cmin⁻¹ under a nitrogen flow rate of 20 mL min⁻¹. Weight losses of the film specimens were reported as a function of temperature (Ahmad, Benjakul, Prodpran, & Dubois, 2010).

Microbiological analysis

The disc-diffusion method was employed to determine the antibacterial activity of the films on bacterial strains. The film samples were cut into discs with the diameter of 10 mm. Next, they were placed on the surface of MHA plates. The medium had been previously smeared with 0.1 ml of an overnight broth culture containing approximately 10^8 colony forming units (CFU) per milliliter of the test bacteria. Bacterial strains were subsequently incubated at 37°C for 24 h. The diameter of the inhibition zone was measured with a caliper to the nearest 0.02 mm and recorded in millimeters. A film without essential oil was applied as control in parallel. The clear zones surrounding the film discs were measured as the inhibition zone (annular radius) indicating the antimicrobial activity (Dashipour et al., 2015).

Statistical analysis

Mean ±standard deviation was obtained using the GLM procedure in SAS statistical software (Version 9.1; Statistical Analysis System Institute Inc., Cary, NC, USA). Significant differences between the means were detected by the Duncan's multiple range test at the confidence level of P< 0.05.

Results and Discussion

Physical properties

The effects of incorporating SEO on the physical properties of chitosan- based nanocomposite films are reported in Table 1. Film thickness varied between 0.141 and 0.190 mm. The thickness of the control film (without essential oil) was 0.141 mm; these were increased significantly (*P<0.05*) as SEO content was increased. This increase was probably due to the entrapment of SEO microdroplets within the polymer matrix. A similar trend was observed when *Zataria multiflora* essential oil was added to carboxymethyl cellulose film (Dashipour *et al*., 2014). The solubility of the bionanocomposite films as a function of SEO content is shown in Table 1. In this study, chitosan-based nanocomposite film showed a low solubility value (18.18±0.94) after 6 h of dipping which was similar to the value (15.03±0.96 %) reported by (Abdollahi *et al*., 2012). When SEO was added, a significant

(P<0.05) decrease was observed in water solubility. By increasing the SEO concentration from 0.5 to 2% in film solutions, WS was decreased significantly (P<0.05) from 18.18 to 13.10. This might attributed to the hydrophobic nature of SEO as well as the formation of intermolecular interactions between essential oil constituents and the hydroxyl groups of chitosan matrix−(Atef *et al*., 2014, Salarbashi *et al*., 2013, Shojaee-Aliabadi *et al.,* 2013).

Table 1. Physical and mechanical properties of chitosan-based nanocomposite films incorporated with SEO.

SEO (% v/v)	Thickness (mm)	Solubility in water (%)	WVP (g s^{-1} m^{-1} Pa^{-1} × 10^{-10})	TS (MPa)	EAB (%)
0.0	0.141 ± 0.003[d]	18.18 ± 0.94[a]	0.64 ± 0.04[d]	27.76 ± 2.13[a]	38.61 ± 1.27[c]
0.5	0.153 ± 0.004[c]	17.40 ± 0.72[a]	0.76 ± 0.05[c]	26.03 ± 1.05[a]	39.29 ± 1.77[bc]
1	0.166 ± 0.002[b]	15.56 ± 0.32[b]	0.92 ± 0.07[b]	23.14 ± 0.85[b]	41.90 ± 0.98[b]
2	0.190 ± 0.003[a]	13.10 ± 0.79[c]	1.23 ± 0.05[a]	16.05 ± 0.73[c]	44.72 ± 1.41[a]

Values within each column with different letters are significantly different ($P < 0.05$).

Water vapor permeability

WVP values of chitosan-MMT films containing SEO at various concentrations are summarized in Table 1. The results revealed that an increase in SEO content increased the WVP value (P<0.05). The WVP was 0.64×10^{-10} g s^{-1} m^{-1} Pa^{-1} for the control film (without essential oil), which was increased to 1.23×10^{-10} gs^{-1}m^{-1}Pa^{-1} for the nano composites that contained 2% SEO. Although the presence of SEO microdroplets increase the hydrophobicity ratio of the films, it caused an increase in the moisture passing through the film as well. This can be attributed to the negative effect of SEO incorporation on the cohesion forces of the polymer matrix. Similar results have been reported by Bonilla *et al*. (2012) in chitosan based films containing basil and thyme essential oils and in quince seed mucilage based films containing oregano essential oil (Jouki, Yazdi, Mortazavi, & Koocheki, 2014). They showed that the rise in basil, thyme and oregano essential oils concentration, led to an increase in WVP values.

Mechanical properties

Stress−strain test is one of the most important tests in packaging materials and may contribute to the estimation and prediction of their mechanical properties in food applications (Ghasemlou, Khodaiyan, & Oromiehie, 2011). The effect of various SEO incorporations on the mechanical properties of the film samples is presented in Table 1. The results demonstrated that SEO significantly (P<0.05) affected the tensile strength and extensibility of the nanocomposite films. The TS was 27.76 MPa for the control film and was decreased significantly (P<0.05) to 16.05 MPa for the films containing 2% SEO. The results are in agreement with the previously published literature (Sánchez-González, Gonzalez- Martinez, Chiralt, & Chafer, 2010). Conversely, EAB of the nanocomposite films was increased significantly from 38.61% to 44.72% (P<0.05). Since the essential oil acted as plasticizer and increased the extensibility of the polymer chains. Addition of essential oil to the film can result in the formation of a weak network structure (Atef *et al*., 2015). A similar trend was reported by Hosseini *et al*. (2015) on fish gelatin− chitosan films incorporated with *Origanum vulgare* L. essential oil.

Optical properties

Optical properties are important factors in terms of general appearance and consumer acceptance (Abdollahi *et al*., 2012). Table 2 shows the color values (L, a, b), total color difference (ΔE) and whiteness index (WI) of the nanocomposite films and those containing SEO. Films without SEO were clear and had a transparent appearance (higher L value). However, the films containing SEO had a slightly yellow appearance, as demonstrated by a remarkable increase in the yellow/blue (b) value and total color difference (ΔE).

Nevertheless, a decrease was observed in the lightness (L), red/green (a), and whiteness index (WI) values as a function of SEO content. Similar results were observed for agar- cellulose bionanocomposite films containing savory essential oil (Atef *et al.*, 2015). This phenomenon is probably due to the presence of phenolic compounds in SEO, which might have light absorbance at low wavelengths. The films incorporated with SEO

showed a markedly ($p<0.05$) greater total color difference (ΔE) in comparison to the control films; this could be ascribed to the decrease in brightness (L*) and the increase observed in the colorimetric coordinate (b*). Similar results were observed by Benavides *et al.* (2012) when oregano essential oil was added to the alginate film.

Table 2. Effect of various concentrations of SEO on color parameters of chitosan-based nanocomposite films.

SEO (% v/v)	L	a	b	ΔE	WI
0.0	85.51 ± 0.13^a	-1.54 ± 0.09^a	7.70 ± 0.04^d	10.79 ± 0.13^d	83.52 ± 0.12^a
0.5	83.29 ± 0.58^b	-2.73 ± 0.03^b	12.09 ± 0.75^c	15.14 ± 0.91^c	79.19 ± 0.89^b
1	81.98 ± 1.60^b	-3.04 ± 0.14^c	14.57 ± 1.73^b	17.78 ± 2.36^b	76.62 ± 2.33^c
2	79.65 ± 0.19^c	-3.27 ± 0.29^c	17.53 ± 0.52^a	21.50 ± 0.41^a	72.94 ± 0.40^d

Values within each column with different letters are significantly different ($P < 0.05$).

X-ray diffraction (XRD)

X-ray diffractograms of chitosan, pure nano-MMT and chitosan/MMT nano

composite films with and without SEO are depicted in Fig. 1.
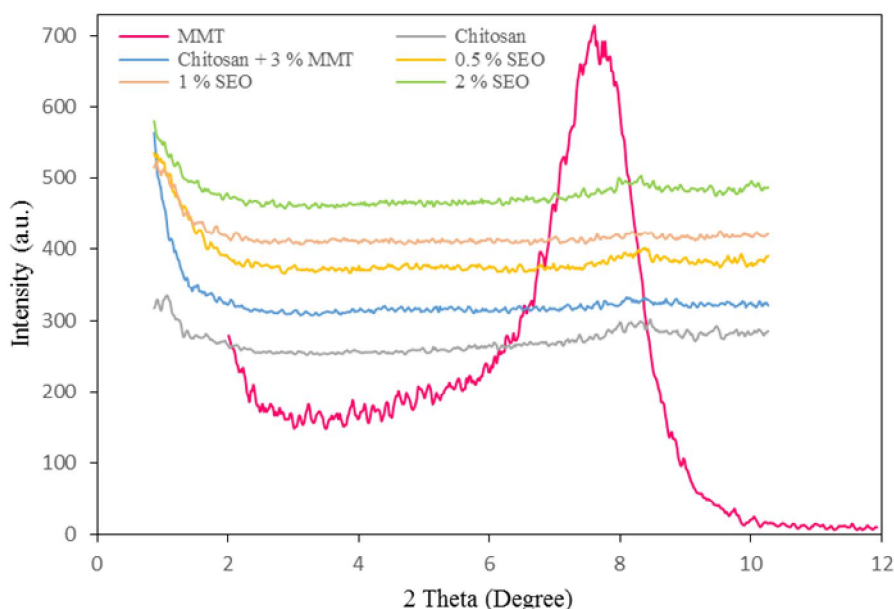

Fig 1. XRD patterns for the pristine MMT and chitosan-based nanocomposite films incorporated with various concentrations of SEO.

During intercalation, insertion of polymer chains into the MMT layers forced the platelets apart and increased the d-spacing. This created a shift in the diffraction peak of montmorillonite toward lower angles

regardless of the clay content (Xu *et al.*, 2006). In an exfoliated (or delaminated) nanocomposite structure, diffraction peaks of nano-clay disappear from the XRD patterns due to the lack of order between the silicate

layers (Alexandre & Dubois, 2000). The crystalline structure of chitosan is strongly dependent on its processing condition, as well as its origin and molecular constitution, such as its molecular weight and degree of deacetylation (Lavorgna, Piscitelli, Mangiacapra, & Buonocore, 2010). Pure chitosan films showed a characteristic crystallinity peak at around 2θ=8.42° which was also observed in the nanocomposite films. As can be seen in Fig. 1, the crystallinity of chitosan was slightly reduced by the incorporation of MMT clay. Previous studies on the chitosan films (Abdollahi *et al.* 2012) containing MMT, have presented similar trends. MMT exhibited a single diffraction peak at (2θ=7.61°). The reflection peak was disappeared with the incorporation of 3 wt % MMT into the chitosan solution, indicating the formation of an exfoliated structure (homogeneously dispersed structure) that was disordered and not detectable by XRD (Xu *et al.* 2006). Moreover, addition of SEO at various concentrations did not affect the structure of chitosan/MMT films. Similar results were reported for chitosan/clay nanocomposite films incorporated with rosemary essential oil (Abdollahi *et al.* 2012) and agar/cellulose nanocomposite films formulated with savory essential oil (Atef *et al.* 2015).

Film microstructure

Scanning electron microscopy (SEM) allows the microstructural analysis of films and provides a better understanding of the relationships between water vapor transmission mechanisms, mechanical and optical properties with the film structural characteristics. Fig. 2 illustrates SEM micrographs of the surface and cross-section of the films.
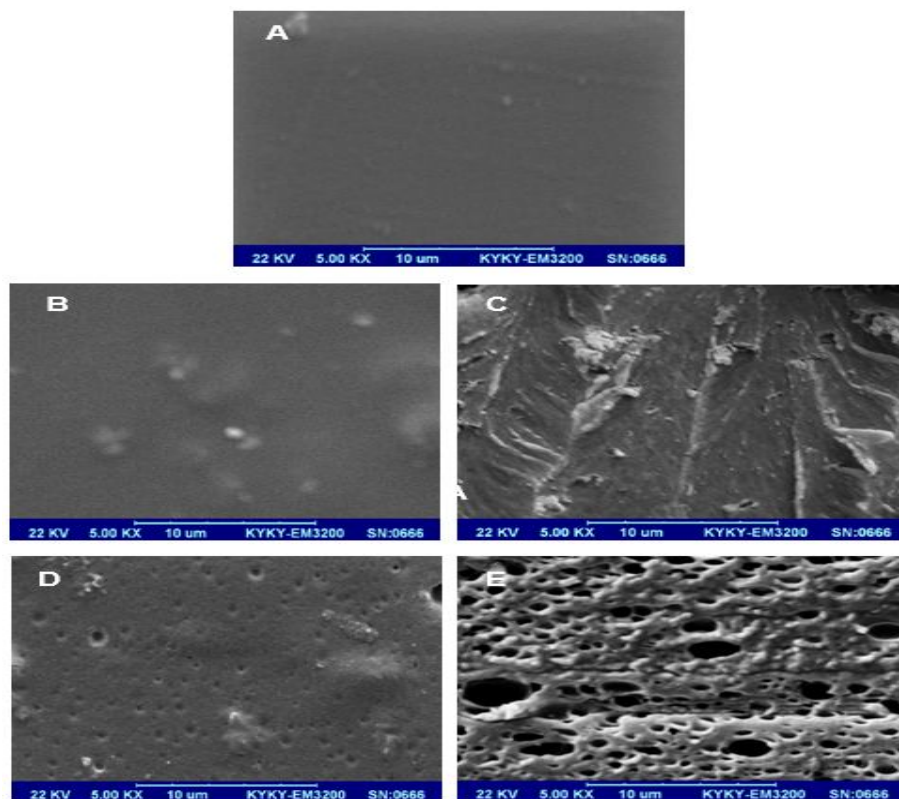

Fig. 2. SEM images of the surface (A: pure chitosan, B-C: chitosan-MMT, D: chitosan- MMT containing 2% SEO) and cross-section (D) of chitosan-MMT film containing 2% SEO.

The pure chitosan film had a compact, smooth and continuous surface (Fig. 2 A). As

seen, chitosan/MMT film had a compact, homogenous and continuous structure without irregularities, cracks or pores. This indicated that MMT nanoparticles were approximately well-dispersed in the chitosan matrix (Fig. 2 B-C). The surface and cross-section of film containing SEO were covered with micro-pores and seemed to be sponge-like (Fig. 2 D-E). Essential oil might have been evaporated during drying (Ahmad *et al.* 2012) leading to the formation of micro-pores throughout the film. Microscopy image revealed that the presence of SEO caused a heterogeneous structure in which oil droplets were entrapped in the continuous carbohydrate network. This could be due to the negative effect of oil

incorporation on the cohesion forces of the chitosan matrix, which enhance transparent phenomena through the film (bonilla *et al.*, 2012, Hosseini *et al.*, 2009). Thus, film microstructure might be associated with the attributes of the film, particularly water vapor permeability of the resulting film.

Thermo-gravimetric analysis (TGA)

TGA thermograms representing the thermal degradation behavior of chitosan nanocomposite films incorporated with SEO at different concentrations are illustrated in Fig. 3. The degradation temperatures (Td), weight loss (Δw) and residue of the film samples are presented in Table 3.

Table 3. Thermal degradation temperature (Td, ∘C) and weight loss (Δw, %) of chitosan-based nanocomposite films incorporated with various concentrations of SEO.

SEO (% v/v)	Δ 1		Δ 2		Δ 3		Δ 4		Residue (%)
	Td_1	Δw_1	Td_2	Δw_2	Td_3	Δw_3	Td_4	Δw_4	
0.0	117.5	11.52	226.66	20.46	316.66	43.66	-	-	24.36
0.5	115.83	10.42	235.83	18.83	313.33	35.10	424.16	16.52	19.13
1	110.83	9.20	240	18.45	322.5	36.62	430.83	15.58	20.15
2	114.16	7.88	241.66	17.01	325	37.21	433.33	16.48	21.42

Δw_1, Δw_2, Δw_3 and Δw_4 indicate the first, second, third and fourth stage weight loss, respectively, of film during TGA heating scan.
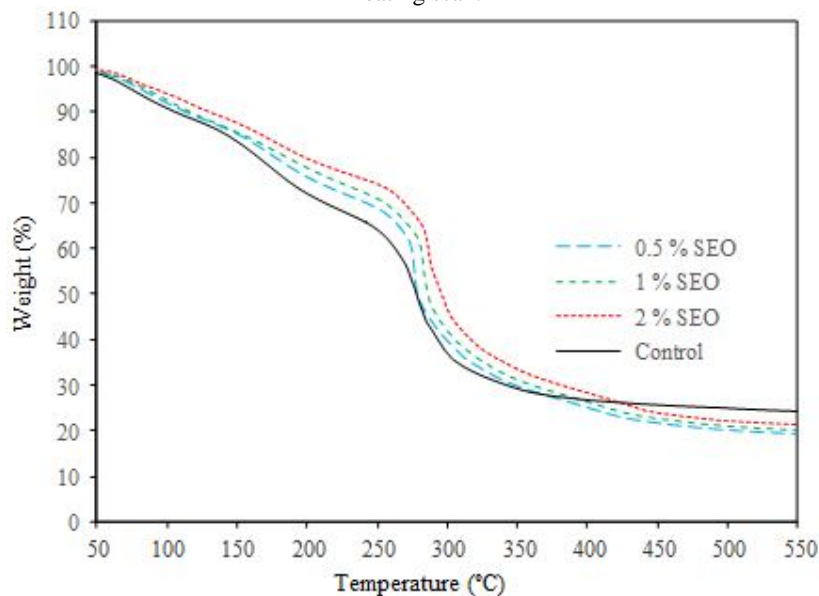

Fig 3. TGA graph of chitosan-based nanocomposite films incorporated with various concentrations of SEO.

The control chitosan film exhibited three main stages of weight loss. A similar result

was observed in the chitosan film (Shen *et al.* 2015). However, four main stages of weight loss were found in the films incorporated with SEO. The first stage of weight loss (Δw_1=7.88–11.52%), observed over the onset temperature (Td_1) ranging from 110.83 to 117.50°C, is mostly associated with the evaporation of residual water and the acetic acid in the film. The second stage of weight loss (Δw_2=17.01–20.46%) was appeared at Td_2 of 226.66–241.66°C. This stage of weight loss was possibly caused by the degradation of lower molecular weight components or structurally bound water in the chitosan network. The third stage of weight loss, Δw_3 of 35.10–43.66% and Td_3 of 313.13–325°C which was obtained for all film samples, mostly associated with the dehydration of saccharide rings, de-polymerization and pyrolytic decomposition of the acetylated and deacetylated units of the polysaccharide (Abdollahi, Rezaei, & Farzi, 2012). In general, the thermal degradation temperature of the second and third stages for all films containing SEO was higher than the control film. With the increase of SEO level in the films, the degradation temperature was enhanced but the weight loss decreased. An enhanced thermal stability of the chitosan samples with SEO was attributed to the interaction between chitosan and SEO, yielding a stronger polymer matrix, thus leading to the higher thermal resistance of the resulting film compared with the pure chitosan film. In the fourth stage of weight loss, Δw_4 of 15.58–16.52% and Td_4 of 424.16–433.33°C was obtained for the films containing SEO. Nevertheless, this stage (Δw_4) was disappeared for the pure chitosan film. It was noted that this stage was likely associated with the loss of the thermally stable components of SEO incorporated in the polymer matrix. Overall, lower residue (or char content) from thermal degradation was observed in SEO-containing films, compared with the control film. TGA curves showed clearly that SEO at different concentrations contributed to a substantial improvement in the thermal stability of the chitosan film.

Antibacterial activity

The antimicrobial activity of the nanocomposite films incorporated with SEO at various concentrations against the selected microorganisms is shown in Table 4. The chitosan/MMT nanocomposite film without SEO served as the control sample that did not show any antibacterial effect against all studied bacterial strains, resulting in no inhibition zones (Table 4). The results were in concordance with those of (Hosseini, Razavi, & Mousavi, 2009) who reported that the chitosan films showed no antibacterial effect against *Listeria monocytogenes*, *Staphylococcus aureus*, *Salmonella enteritidis* and *Pseudomonas aeroginosa*. According to Coma *et al.*, (2002), chitosan does not diffuse through the adjacent agar media in the agar diffusion method, as only organisms in direct contact with the active sites of chitosan are inhibited. Using the direct-contact test, the films containing 1% (v/v) SEO were not effective against *S. typhimurium*, yet exhibited a certain antibacterial effect on the growth of *B. cereus*, *S. aureus* and *E. coli* as evidenced by minimal bacterial growth around the film discs. As the concentration of SEO was increased, the zone of inhibition also was increased significantly (P<0.05). Among the examined bacteria, *S. typhimurium* and *S. aureus* were the most resistant and most susceptible to SEO-containing films, respectively. In accordance with these results, Shojaee-Aliabadi *et al.* (2012) reported that k-carrageenan films produced with *Satureja hortensis* essential oil showed a greater inhibition zone for *S. aureus* than *B. cereus*, *E. coli*, *S. typhimurium* and *P. aeruginosa*. The antibacterial effect of SEO is attributed to its relatively high concentration of carvacrol, γ–terpinene and p-cymene (Hadian *et al.*, 2010). These constituents can disintegrate the external membrane of gram-negative bacteria, and thus increase the permeability of the cytoplasmic membrane (Burt, 2004). In general, SEO-containing films were obviously more effective against gram-positive bacteria than the gram-negative ones. This might be due to the impermeable outer membrane

surrounding gram negative bacteria (Fisher &   Phillips, 2006).

Table 4. Antimicrobial activity of chitosan-based nanocomposite films incorporated with various concentrations of SEO.

SEO (% v/v)	Inhibition zone (mm^2)			
	S. aureus	*B. cereus*	*E. coli*	*S. typhimurium*
0.0	0.00[c]	0.00[c]	0.00[c]	0.00[b]
0.5	0.00[c]	0.00[c]	0.00[c]	0.00[b]
1	45.71 ± 6.13[b]	29.58 ± 4.25[b]	18.73 ± 3.10[b]	0.00[b]
2	144.85 ± 12.97[a]	98.40 ± 8.14[a]	83.62 ± 7.82[a]	65.12 ± 5.36[a]

Values within each column with different letters are significantly different ($P < 0.05$).

Conclusions

The incorporation of SEO into the chitosan-based nanocomposite film was successfully performed to prepare antimicrobial biodegradable films. Addition of SEO significantly influenced the properties of the resulting films. The incorporation of SEO into the film decreased tensile strength and water solubility, while increased the percentage of EAB, WVP as well as the thickness of the nanocomposite films. Scanning electron microscopy showed that the microstructure of emulsified films had a critical effect on their WVP and mechanical properties. The obtained results indicated that SEO at various concentrations led to different thermal resistance for the resulting films. The films exhibited highest inhibition against gram-positive bacteria (*S. aureus* and *B. cereus*) than gram-negative bacteria (*S. typhimurium* and *E. coli*). Overall, this study demonstrates that SEO-containing films present a good potential for being applied in food packaging. Although further studies, such as analysis of the physical stability and inhibition against other harmful microorganisms, are still needed.

Acknowledgment

References

Abdollahi, M., Rezaei, M., & Farzi, G. (2012). A novel active bionanocomposite film incorporating rosemary essential oil and nanoclay into chitosan. *Journal of Food Engineering*, 111(2), 343-350.

Ahmad, M., Benjakul, S., Prodpran, T., & Agustini, T. W. (2012). Physico-mechanical and antimicrobial properties of gelatin film from the skin of unicorn leatherjacket incorporated with essential oils. *Food Hydrocolloids*, 28(1), 189-199.

Alexandre, M., & Dubois, P. (2000). Polymer-layered silicate nanocomposites: preparation, properties and uses of a new class of materials. *Materials Science and Engineering*: R: Reports, 28(1), 1-63.

Almasi, H., Ghanbarzadeh, B., & Entezami, A. A. (2010). Physicochemical properties of starch–CMC–nanoclay biodegradable films. International *Journal of Biological Macromolecules*, 46(1), 1-5.

ASTM. (2002). Standard test method for tensile properties of thin plastic sheeting. In Annual book of ASTM standards designation D882. Philadelphia, PA: American Society for Testing and Materials.

Atef, M., Rezaei, M., & Behrooz, R. (2015). Characterization of physical, mechanical, and antibacterial properties of agar-cellulose bionanocomposite films incorporated with savory essential oil. *Food Hydrocolloids*, 45, 150-157.

Avella, M., De Vlieger, J. J., Errico, M. E., Fischer, S., Vacca, P., & Volpe, M. G. (2005).

Biodegradable starch/clay nanocomposite films for food packaging applications. *Food Chemistry*, 93(3), 467-474.

Benavides, S., Villalobos-Carvajal, R., & Reyes, J. E. (2012). Physical, mechanical and antibacterial properties of alginate film: effect of the crosslinking degree and oregano essential oil concentration. *Journal of Food Engineering*, 110(2), 232-239.

Bonilla, J., Atarés, L., Vargas, M., & Chiralt, A. (2012). Effect of essential oils and homogenization conditions on properties of chitosan-based films. *Food Hydrocolloids*, 26(1), 9-16.

Burt, S. (2004). Essential oils: their antibacterial properties and potential applications in foods—a review. *International Journal of Food Microbiology*, 94(3), 223-253.

Coma, V., Martial-Gros, A., Garreau, S., Copinet, A., Salin, F., & Deschamps, A. (2002). Edible antimicrobial films based on chitosan matrix. *Journal of Food Science*, 67(3), 1162-1169.

Dashipour, A., Razavilar, V., Hosseini, H., Shojaee-Aliabadi, S., German, J. B., Ghanati, K., ... & Khaksar, R. (2015). Antioxidant and antimicrobial carboxymethyl cellulose films containing Zataria multiflora essential oil. *International ournal of Biological Macromolecules*, 72, 606-613.

Fisher, K., & Phillips, C. A. (2006). The effect of lemon, orange and bergamot essential oils and their components on the survival of *Campylobacter jejuni*, *Escherichia coli* O157*, Listeria monocytogenes*, *Bacillus cereus* and *Staphylococcus aureus* in vitro and in food systems. *Journal of Applied Microbiology*, 101(6), 1232-1240.

Gennadios, A., Hanna, M. A., & Kurth, L. B. (1997). Application of edible coatings on meats, poultry and seafoods: a review. *LWT-Food Science and Technology*, 30(4), 337-350.

Ghasemlou, M., Khodaiyan, F., & Oromiehie, A. (2011). Physical, mechanical, barrier, and thermal properties of polyol-plasticized biodegradable edible film made from kefiran. *Carbohydrate Polymers*, 84(1), 477-483.

Hadian, J., Ebrahimi, S. N., & Salehi, P. (2010). Variability of morphological and phytochemical characteristics among Satureja hortensis L. accessions of Iran. *Industrial Crops and Products*, 32(1), 62-69.

Hosseini, M. H., Razavi, S. H., & Mousavi, M. A. (2009). Antimicrobial, physical and mechanical properties of chitosan-based films incorporated with thyme, clove and cinnamon essential oils. *Journal of Food Processing and Preservation*, 33(6), 727-743.

Hosseini, S. F., Rezaei, M., Zandi, M., & Farahmandghavi, F. (2015). Bio-based composite edible films containing Origanumvulgare L. essential oil. *Industrial Crops and Products*, 67, 403-413.

Jouki, M., Yazdi, F. T., Mortazavi, S. A., & Koocheki, A. (2014). Quince seed mucilage films incorporated with oregano essential oil: physical, thermal, barrier, antioxidant and antibacterial properties. *Food Hydrocolloids*, 36, 9-19.

Lavorgna, M., Piscitelli, F., Mangiacapra, P., & Buonocore, G. G. (2010). Study of the combined effect of both clay and glycerol plasticizer on the properties of chitosan films. *Carbohydrate Polymers*, 82(2), 291-298.

Peng, Y., & Li, Y. (2014). Combined effects of two kinds of essential oils on physical, mechanical and structural properties of chitosan films. *Food Hydrocolloids*, 36, 287-293.

Salarbashi, D., Tajik, S., Shojaee-Aliabadi, S., Ghasemlou, M., Moayyed, H., Khaksar, R., & Noghabi, M. S. (2014). Development of new active packaging film made from a soluble soybean polysaccharide incorporated Zataria multiflora Boiss and Mentha pulegium essential oils. *Food Chemistry*, 146, 614-622.

Sánchez-González, L., González-Martínez, C., Chiralt, A., & Cháfer, M. (2010). Physical and antimicrobial properties of chitosan–tea tree essential oil composite films. *Journal of Food Engineering*, 98(4), 443-452.

Sefidkon, F., Abbasi, K., & Khaniki, G. B. (2006). Influence of drying and extraction methods on yield and chemical composition of the essential oil of *Satureja hortensis*. *Food Chemistry*, 99(1), 19-23.

Shen, Z., & Kamdem, D. P. (2015). Development and characterization of biodegradable chitosan films containing two essential oils. *International Journal of Biological Macromolecules*, 74, 289-296.

Shojaee-Aliabadi, S., Hosseini, H., Mohammadifar, M. A., Mohammadi, A., Ghasemlou, M., Ojagh, S. M., & Khaksar, R. (2013). Characterization of antioxidant-antimicrobial κ-carrageenan films containing Satureja hortensis essential oil. *International Journal of Biological Macromolecules*, 52, 116-124.

Wang, S. F., Shen, L., Tong, Y. J., Chen, L., Phang, I. Y., Lim, P. Q., & Liu, T. X. (2005). Biopolymer chitosan/montmorillonite nanocomposites: preparation and characterization. *Polymer Degradation and Stability*, 90(1), 123-131.

Xu, Y., Ren, X., & Hanna, M. A. (2006). Chitosan/clay nanocomposite film preparation and characterization. *Journal of Applied Polymer Science*, 99(4), 1684-1691.

Zolfi, M., Khodaiyan, F., Mousavi, M., & Hashemi, M. (2014). The improvement of characteristics of biodegradable films made from kefiran–whey protein by nanoparticle incorporation. *Carbohydrate polymers*, 109, 118-125.

تولید و ارزیابی فیلم نانوکامپوزیتی کیتوزان- مونت‌موریلونیت حاوی اسانس

مرزه (*Satureja hortensis*)

وحید علیزاده[1]- حسن برزگر[2]*- بهزاد ناصحی[3]- وحید سمواتی[2]

چکیده

در تحقیق حاضر، خصوصیات فیزیکوشیمیایی و ضدمیکروبی فیلم‌های فعال نانوکامپوزیتی کیتوزان-نانورس حاوی مقادیر مختلف اسانس مرزه (0/5، 1 و 2 درصد حجمی/ حجمی) مورد ارزیابی قرار گرفت. با افزودن اسانس به فیلم‌ها، مقاومت به کشش، کاهش و کشش‌پذیری فیلم‌ها، به‌طور معنی‌داری افزایش پیدا کرد. نتایج نشان داد که از بین نمونه‌های فیلم مورد آزمون، فیلم شاهد دارای کمترین میزان نفوذپذیری نسبت به عبور بخار آب بود. همچنین با افزایش غلظت اسانس، حلالیت در آب و شفافیت فیلم‌ها کاهش یافت. نتایج آزمون گرما وزن‌سنجی (TGA) نشان داد که فیلم‌های حاوی اسانس مرزه نسبت به فیلم شاهد دارای دمای تخریب بالاتری هستند. در ادامه خصوصیات ساختاری و مورفولوژیکی فیلم‌های نانوکامپوزیتی، بوسیله روش پراش پرتو ایکس (XRD) و میکروسکوپ الکترونی روبشی (SEM) مورد بررسی قرار گرفت. فیلم‌های حاوی اسانس مرزه، روی باکتری‌های گرم مثبت (*Bacillus cereus* و *Staphylococcus aureus*) نسبت به باکتری‌های گرم منفی (*Escherichia coli* و *Salmonella typhimurium*) تاثیر بازدارندگی بیشتری داشتند. در نهایت نتایج نشان داد که اسانس مرزه می‌تواند به‌عنوان یک ماده ضدباکتری طبیعی در ساخت فیلم‌های زیست تخریب پذیر ضدمیکروب مورد استفاده قرار گیرد.

واژه‌های کلیدی: فیلم نانوکامپوزیتی، کیتوزان، مرزه، روغن اساسی، ضدمیکروب.